# Electron and Proton Transfer in the Arginine-54-Methionine Mutant of Cytochrome *c* Oxidase from *Paracoccus denitrificans*†

Audrius Jasaitis, Camilla Backgren, Joel E. Morgan,‡ Anne Puustinen, Michael I. Verkhovsky, and Mårten Wikström*

*Helsinki Bioenergetics Group, Department of Medical Chemistry, Institute of Biomedical Sciences and Biocentrum Helsinki, P.O. Box 8, University of Helsinki, FI-00014 Helsinki, Finland*

*Received December 27, 2000*

ABSTRACT: Arginine 54 in subunit I of cytochrome *c* oxidase from *Paracoccus denitrificans* interacts with the formyl group of heme *a*. Mutation of this arginine to methionine (R54M) dramatically changes the spectral properties of heme *a* and lowers its midpoint redox potential [Kannt et al. (1999) *J. Biol. Chem. 274*, 37974−37981; Lee et al. (2000) *Biochemistry 39*, 2989−2996; Riistama et al. (2000) *Biochim. Biophys. Acta 1456*, 1−4]. During anaerobic reduction of the mutant enzyme, a small fraction of heme *a* is reduced first along with heme $a_3$, while most of heme *a* is reduced later. This suggests that electron transfer is impaired thermodynamically due to the low redox potential of heme *a* but that it still takes place from $Cu_A$ via heme *a* to the binuclear site as in wild-type enzyme, with no detectable bypass from $Cu_A$ directly to the binuclear site. Consistent with this, the proton translocation efficiency is unaffected at 1 $H^+/e^-$ in the mutant enzyme, although turnover is strongly inhibited. Time-resolved electrometry shows that when the fully reduced enzyme reacts with $O_2$, the fast phase of membrane potential generation during the $\mathbf{P_R} \rightarrow \mathbf{F}$ transition is unaffected by the mutation, whereas the slow phase ($\mathbf{F} \rightarrow \mathbf{O}$ transition) is strongly decelerated. In the $3e^-$-reduced mutant enzyme heme *a* remains oxidized due to its lowered midpoint potential, whereas $Cu_A$ and the binuclear site are reduced. In this case the reaction with $O_2$ proceeds via the $\mathbf{P_M}$ state because transfer of the electron from $Cu_A$ to the binuclear site is delayed. The single phase of membrane potential generation in the $3e^-$-reduced mutant enzyme, which thus corresponds to the $\mathbf{P_M} \rightarrow \mathbf{F}$ transition, is decelerated, but its amplitude is comparable to that of the $\mathbf{P_R} \rightarrow \mathbf{F}$ transition. From this we conclude that the completely ($4e^-$) reduced enzyme is fully capable of proton translocation.

The electron-transfer pathway in the cytochrome *c* oxidases has usually been considered to strictly follow the sequence $Cu_A \rightarrow$ heme *a* $\rightarrow$ binuclear center, where the binuclear center of $O_2$ reduction consists of heme $a_3$ and the $Cu_B$ ion next to it and where $Cu_A$ is the entry port of electrons into the enzyme from cytochrome *c* (see refs *1*−*3*). However, from time to time there have been suggestions of direct electron transfer from the $Cu_A$ center to the binuclear site, bypassing heme *a*. Recently, Kannt et al. (*4*) suggested such a bypass in the R54M mutant of subunit I in cytochrome *c* oxidase from *Paracoccus denitrificans*. In this mutant enzyme the strong interaction of arginine-54 with the formyl group of heme *a* is destroyed, which leads to a dramatic lowering of the midpoint redox potential ($E_{m,7}$)[1] of this heme, a large blue shift in its optical spectrum, and strong inhibition of enzyme activity (*4*, *5*). Lee et al. (*6*) reported similar changes in the corresponding R52A mutant of cytochrome *c* oxidase from *Rhodobacter sphaeroides* and showed a large change in the formyl stretching mode of heme *a* by resonance Raman spectroscopy, proving a hydrogen-bonding interaction between the formyl group and the arginine. In 1983, Babcock and Callahan (*7*) had suggested, on the basis of the optical and Raman properties of heme *a*, that its formyl group is hydrogen-bonded to an amino acid side chain.

In the past, there have been suggestions that the fully reduced cytochrome *c* oxidase may yield only incomplete proton translocation upon its oxidation by $O_2$, in line with the assumption that this state of the enzyme would have minimal occupancy under aerobic conditions in vivo. More specifically, it has been proposed that proton translocation associated with the first reactions of the fully reduced enzyme with $O_2$, after formation of the dioxygen adduct, may be bypassed (*2*, *8*, *9*). In contrast to this, we have recently shown that oxidation of the fully reduced enzyme by $O_2$, followed by its immediate rereduction, yields translocation of four protons, i.e., the full complement of proton pumping (*10*). This question is an important issue with regard to the interpretation of several kinds of experiments that start out with fully reduced cytochrome *c* oxidase, e.g., measurements of proton ejection and formation of membrane potential ($\Delta\psi$).

† This work is dedicated to the memory of Dr. Gerald T. Babcock (1946-2000) and to his fundamental contributions to research on cytochrome *c* oxidase. Supported by grants from the Academy of Finland (program 44895), the University of Helsinki, Biocentrum Helsinki, and the Sigrid Juselius Foundation.

* Corresponding author. E-mail: Marten.Wikstrom@Helsinki.Fi. Phone: +358-9-191 8260. Fax: +358-9-191 8296.

‡ Present address: Department of Biochemistry, University of Illinois at Urbana-Champaign, A306 CLSL, Mail Code 25-6, 600 S. Mathews Ave., Urbana, IL.

[1] Abbreviations: $E_{m,7}$, midpoint redox potential at pH = 7 (vs NHE); $\Delta\psi$, electrical membrane potential; *k*, rate constant; $\tau$, time constant (1/*k*).

10.1021/bi002948b CCC: $20.00 
Published on Web 04/03/2001

Here, we have set out to analyze the phenotype of the R54M mutant enzyme by optical spectroscopy and time-resolved electrometry. The results show that electron transfer from $Cu_A$ to heme *a* is impaired in the mutant enzyme for thermodynamic reasons but that electron transfer from $Cu_A$ to the binuclear site still takes place via heme *a*. The R54M mutant enzyme was also found to be a valuable tool for assessing whether the proton translocation efficiency is different when the fully and partially reduced enzyme reacts with $O_2$.

## MATERIALS AND METHODS

*Enzyme Preparation.* Site-directed mutagenesis, bacterial growth conditions, and purification of cytochrome $aa_3$ from *P. denitrificans* were as described previously (*11*).

*Reconstitution of the Enzyme into Phospholipid Vesicles.* Cytochrome $aa_3$ was reconstituted into phospholipid vesicles to form proteoliposomes, using a modification of the methodology developed by Rigaud et al. (*12*), as described in Jasaitis et al. (*13*). The sucrose gradient step was omitted, and the isolated cytochrome $aa_3$ was added to a final concentration of 0.5 $\mu$M.

*Proton translocation* was determined at room temperature by the $O_2$ pulse method under constant argon flow as described before (*14*) but omitting *N*,*N*,*N*′,*N*′-tetramethyl-*p*-phenylenediamine. The rate of reduction of ferricytochrome *c* by ascorbate was determined separately by stopped-flow spectrophotometry under the same conditions but in the absence of proteoliposomes. On the basis of this, the kinetics of proton release in this reaction (0.5 $H^+/e^-$) is plotted in Figure 3 after scaling to the measured buffer capacity of the extravesicular space.

*Electrometric Measurements.* The direct, time-resolved electrical measurements are based on a method originally developed by Drachev and co-workers (*15*). In the present system $Ag/AgCl_2$ electrodes record the voltage between the two compartments of a cell, separated by a measuring membrane, which consists of a lipid-impregnated Teflon mesh. Proteoliposomes were fused to this measuring membrane [see Figure 2 in Verkhovsky et al. (*16*)]. The voltage across the measuring membrane follows the $\Delta\psi$ across the proteoliposome membranes proportionally, allowing the kinetics of charge translocation across the latter to be recorded in a time-resolved fashion. The complete measurement and sample preparation procedure is described in Jasaitis et al. (*13*).

*Measurement Electronics.* The electrometric measurement system consisted of a homemade operational preamplifier whose output could be recorded using a 12-bit CompuScope 512 (Gage Applied Sciences, Montreal, Canada) running a data acquisition software written by Nikolai Belevich.

*Optical Flow-Flash.* The kinetics of the reaction of $aa_3$ oxidase with dioxygen were followed on a millisecond time scale at room temperature using the flow-flash technique developed by Gibson and Greenwood (*17*). The CO-inhibited enzyme, at different levels of reduction, was mixed with oxygen-saturated buffer in the dark. The reaction was then initiated by photolyzing CO from the enzyme with a xenon camera flash. To prevent premature photolysis by the probe beam, a camera shutter was used to block the beam until a few milliseconds before the flash. The subsequent reaction was followed optically using a diode array kinetic spectrophotometer made by Unisoku Instruments (Kyoto, Japan). The mixing was done using the RX2000 mixer from Applied Photophysics (Leatherhead, U.K.) with a mixing ratio of 1:1.

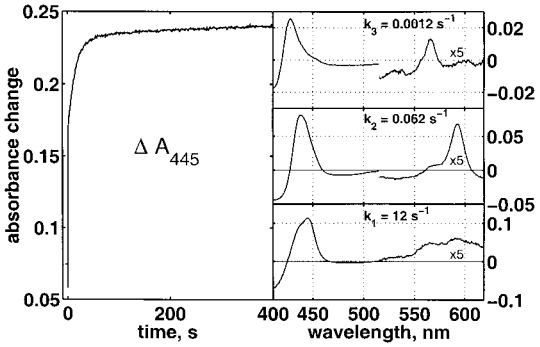


FIGURE 1: Kinetics of heme reduction in the R54M mutant enzyme. Stopped-flow experiment with 0.2 M HEPES (pH 8), 0.05% dodecyl maltoside, 10 $\mu$g/mL catalase, and 3.5 $\mu$M R54M mutant enzyme in one syringe and with 0.2 M HEPES (pH 8), 0.05% dodecyl maltoside, 0.4 mM ruthenium(II) hexammine, and 10 mM sodium dithionite in the other. Mixing volume ratio 1:1. Left panel: kinetic trace of enzyme reduction measured at 445 nm. Right panel: Spectra of kinetic components of enzyme reduction obtained by global multiexponential fitting of the data surface (see Materials and Methods).

## RESULTS AND DISCUSSION

We first set out to measure the kinetics of reduction of the oxidized R54M mutant enzyme with dithionite, using ruthenium(II) hexammine as a redox mediator. In such conditions, the redox centers of the enzyme are reduced in an order essentially determined by their relative midpoint redox potentials ($E_{m,7}$), high-potential centers being reduced before low-potential centers. Figure 1 (left panel) shows the kinetics of reduction at 445 nm. A relatively fast phase of reduction is followed by two slower phases. The spectra of these three reduction phases are shown in the right panel. The fastest phase ($k = 12$ s$^{-1}$) can mainly be attributed to reduction of heme $a_3$ from its absorption maximum at 445 nm in the Soret and its broad low-intensity band around 600 nm. This is in contrast with the wild-type enzyme where heme *a* is reduced first, in milliseconds, long before reduction of heme $a_3$ (not shown; cf. ref *18*). However, as Figure 1 shows, the 12 s$^{-1}$ phase clearly includes a small fraction of heme *a* reduction, the absorption peaks of which are shifted to ca. 590 and 439 nm in the R54M mutant enzyme (*4*−*6*). The main part of heme *a* reduction takes place in the second phase ($k = 0.062$ s$^{-1}$), whereas the slowest phase ($k = 0.0012$ s$^{-1}$) is due to reduction of heme *o* (Figure 1; right panels). Heme *o* replaces heme *a* in about one-half of the mutant enzyme molecules, which results in a cytochrome $oa_3$ complex (*4*). The mutant enzyme preparation can thus be described as an approximately 1:1 mixture of cytochrome $aa_3$ and cytochrome $oa_3$. The results in Figure 1 are in agreement with the lowered $E_{m,7}$ of heme *a* in the $aa_3$ complex due to the mutation (*4*, *5*) and with the observation of a still lower $E_{m,7}$ value for heme *o* in the $oa_3$ complex (*4*). The fact that a small part of heme *a* is reduced together with heme $a_3$ in the first kinetic phase suggests that the reduction of the binuclear site may actually take place by the normal electron-transfer route via heme *a*. While electron transfer from $Cu_A$ to heme *a* is impaired, probably due to

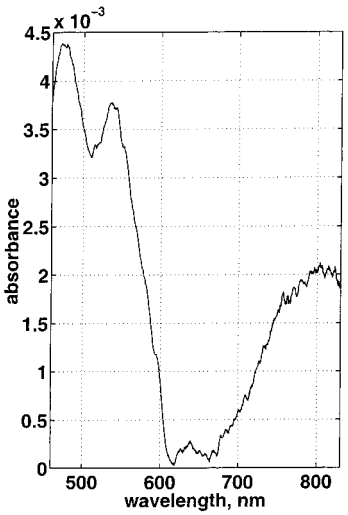


FIGURE 2: Spectrum of oxidized minus reduced $Cu_A$. The spectrum of 2-electron-reduced CO−enzyme minus approximately 3-electron-reduced CO−enzyme was obtained by subtracting the optical spectra at two different time points during the slow reduction of the enzyme by the glucose and glucose oxidase system in the presence of carbon monoxide. Conditions: 0.1 M HEPES (pH 8), 0.1% dodecyl maltoside, 0.5 $\mu$M ruthenium(II) hexammine chloride, 1 atm of CO, and 3 $\mu$M R54M mutant enzyme.

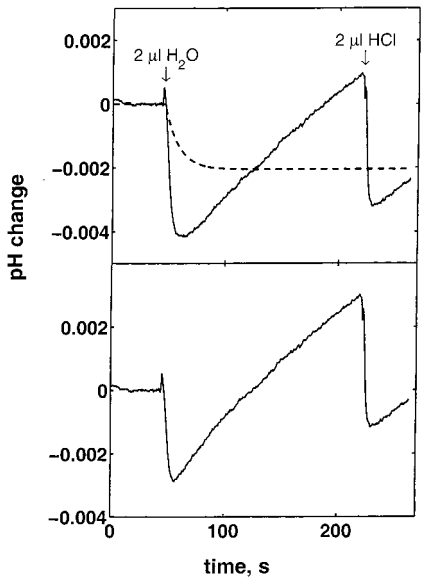


FIGURE 3: Proton translocation by the R54M mutant enzyme. (Top panel) Solid trace: pH response on addition of 2 $\mu$L of air-saturated water and 2 $\mu$L of anaerobic 1 mM HCl. Conditions: 0.1 M KCl, 5 mM potassium ascorbate, 15 $\mu$M cytochrome *c*, 1 $\mu$M valinomycin, and ~0.5 $\mu$M R54M mutant enzyme in proteoliposomes, pH 7.4. Dashed trace: expected release of protons upon reduction of ferricytochrome *c* by ascorbate (see Materials and Methods). (Bottom panel) Solid trace from top panel from which the dashed trace has been subtracted.

the lower driving force, a small part of heme *a* is reduced with the same kinetics as heme $a_3$. The low extent of reduction of heme *a* in the first kinetic phase can be attributed to its low $E_{m,7}$ value relative to heme $a_3$ in the R54M mutant enzyme. It should be emphasized that the reduction of the small fraction of heme *a* together with heme $a_3$ can easily be missed, especially under less reducing conditions. We note that in Figure 5 of Kannt et al. (*4*) a fraction of heme *a* was clearly reduced together with heme $a_3$ in the first spectrum shown and in agreement with the present time-resolved data.

Figure 2 shows another interesting consequence of the uniquely lowered $E_{m,7}$ of heme *a*. Here, the mutant $aa_3$ enzyme is first allowed to form the mixed valence state, where CO stabilizes the reduced forms of heme $a_3$ and $Cu_B$. Upon further reduction, the heme *a* and $Cu_A$ centers become reduced, and in the wild-type enzyme this happens roughly simultaneously due to their similar $E_{m,7}$ values. However, in the mutant enzyme $Cu_A$ is reduced first in a distinct phase, well before reduction of the low-potential hemes *a* and *o*. This makes it possible to record a clean oxidized minus reduced difference spectrum of $Cu_A$ (Figure 2), which is not possible in the wild-type enzyme due to the strongly interferring absorption bands of heme *a*. To our knowledge, this is the first optical difference spectrum of $Cu_A$ recorded over the visible range for the complete enzyme, and it is indeed very similar to previously reported spectra of the separately expressed $Cu_A$ domain of subunit II (*19*).

Although the turnover velocity of the R54M mutant enzyme is low (ca. 20 $s^{-1}$ per $aa_3$; not shown), proton translocation can still be measured by an application of the $O_2$ pulse technique (see Materials and Methods). Figure 3 shows that the $H^+/e^-$ ratio is close to unity, i.e., the same coupling efficiency as in the wild-type enzyme. This observation supports the idea that the mutation specifically affects the rate of the *driving* electron transfer reactions rather than the *driven* proton translocation, or the coupling of the two processes, and it is also in line with the conclusion that electron transfer takes place by the normal route in the mutant. In this connection it may be noted that the conserved residue R54 has been proposed to be part of a proton transfer pathway ("H-channel"; see refs *6* and *20*) that was suggested to be involved in proton translocation by cytochrome *c* oxidase from bovine heart mitochondria (*21*), where R54 corresponds to R38. The observations presented here and in refs *6* and *22*, together with the high degree of homology between the mitochondrial and the bacterial enzymes, are not consistent with this proposal.

The electrometric flow-flash method may be used to determine charge translocation by cytochrome *c* oxidase, which can be kinetically correlated to the individual reaction steps observed in time-resolved optical and Raman measurements of the catalytic cycle (*13*). In brief, the latter measurements (see refs *1*−*3*) have shown that when fully reduced wild-type cytochrome *c* oxidase reacts with $O_2$, formation of the initial dioxygen adduct, compound **A**, is followed by fast ($\tau \sim 30$ $\mu$s) transfer of an electron from heme *a* to the binuclear center. This reaction yields the so-called $\mathbf{P_R}$ state of the binuclear site (*23*), which subsequently relaxes to the ferryl state **F** with $\tau \sim 60$ $\mu$s in the wild-type *Paracoccus* $aa_3$ enzyme (not shown). Roughly simultaneously with this, the electron in $Cu_A$ equilibrates with heme *a*. Transfer of the fourth electron shared between $Cu_A$ and heme *a* to the binuclear site yields the oxidized ferric/cupric form of the site, which is formed with $\tau \sim 1-3$ ms. In contrast, if the reaction is initiated from the so-called mixed valence, 2-electron-reduced state, formation of compound **A** is followed by its decay to the $\mathbf{P_M}$ intermediate at which state the reaction stops. Formation of $\mathbf{P_M}$ is five to six times slower than formation of $\mathbf{P_R}$. Analogously, if the reaction starts off with the 3-electron-reduced enzyme, it is truncated at intermediate **F**.

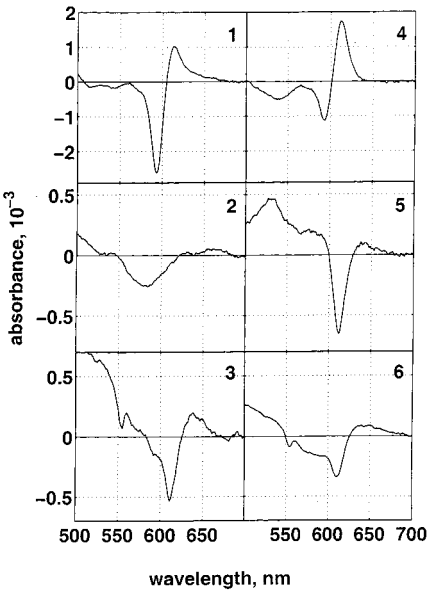


FIGURE 4: Optical changes during the reaction of fully reduced (left panels) and 3-electron-reduced (right panels) R54M mutant enzyme with $O_2$. Spectra of the kinetic components of the flow-flash reaction were obtained by a global exponential fit to the experimental data surfaces. Panels: 1 and 4, change in the spectrum during 1 ms after flashing off CO; 2 and 5, spectra of kinetic components with rate constants of 15 and 93 $s^{-1}$, respectively; 3 and 6, spectra of kinetic components with rate constants of 0.6 and 1.1 $s^{-1}$, respectively. Conditions: syringe 1, 0.1 M HEPES (pH 8), 0.1% dodecyl maltoside, 10 $\mu$g/mL catalase, 55 mM glucose, 12 $\mu$g/mL glucose oxidase, 0.5 $\mu$M ruthenium(II) hexammine chloride, 1 atm of CO, and 3 $\mu$M enzyme; syringe 2, oxygen-saturated 0.1 M HEPES (pH 8) and 0.1% dodecyl maltoside.

Figure 4 shows the spectra of the kinetic components observed in the reaction of the fully reduced (left panels, 1−3) and approximately 3-electron-reduced (right panels, 4−6) R54M mutant enzyme with $O_2$. It is important to stress that the enzyme was reduced in the presence of ruthenium-(II) hexammine and glucose *plus* glucose oxidase. In such conditions the enzyme is reduced very slowly and the redox centers become reduced essentially in the order of their respective $E_{m,7}$ values, as verified by optical difference spectra taken during the process (not shown). It is also important to recall that the mutant enzyme preparation actually contains two types of enzyme, cytochrome $aa_3$ and cytochrome $oa_3$, in roughly equal proportions, as indicated above, and that the $E_{m,7}$ of the heme *o* is extremely low (*4*). Optical spectra taken during reduction of the enzyme indicate that in conditions where the $aa_3$ enzyme fraction is fully reduced, i.e., where even the low-potential heme *a* is reduced, heme *o* in the $oa_3$ enzyme still remains oxidized. Therefore, in panels 1−3 of Figure 4, cytochrome $aa_3$ is fully reduced, but cytochrome $oa_3$ is 3-electron reduced before the reaction with $O_2$. In panels 4−6, both the cytochrome $aa_3$ and cytochrome $oa_3$ fractions of the enzyme are 3-electron reduced (i.e., both heme *a* and heme *o* remain oxidized).

Panels 1 and 4 (Figure 4) are not time-resolved but show the difference spectrum of the events that occur within 1 ms after photolysis of CO in the presence of $O_2$. Extensive oxidation of heme *a* dominates the first phase of the fully reduced enzyme (panel 1). Recall here that the absorption maximum of ferrous *minus* ferric heme *a* is shifted to ca. 590 nm in the R54M mutant enzyme. In addition, there is an absorption peak at ca. 610 nm due to formation of the **P** state *plus*, although less clear (but see below), formation of the **F** state which absorbs maximally at ca. 580 nm. The **P** seen to be formed in the fully reduced case (panel 1) must belong to the $oa_3$ fraction of the mutant enzyme, because this **P** is not seen to relax until the seconds time scale (panel 3). In particular, no relaxation of **P** is seen in the next 50 ms kinetic phase (panel 2). Instead, this phase shows the typical spectrum of relaxation of the **F** state into **O** in the $aa_3$ population. We conclude that when the enzyme with fully reduced $aa_3$ and 3-electron-reduced $oa_3$ (Figure 4, panels 1−3) reacts with $O_2$, both the cytochrome $aa_3$ and cytochrome $oa_3$ fractions in the sample initially form the **P** state. In the $aa_3$ population the formed **P** ($\mathbf{P_R}$) is converted into the **F** state within 1 ms, in accordance with the fact that heme *a* was reduced prior to the reaction with $O_2$. In contrast, the **P** formed in the $oa_3$ population is equivalent to $\mathbf{P_M}$ because there is no electron available in the low-potential heme *o*. The $\mathbf{P_M}$ state of the $oa_3$ population remains stable for seconds because electron transfer from $Cu_A$ to the binuclear site is strongly impeded by the energetically very unfavorable transfer of an electron from $Cu_A$ to the binuclear center via heme *o*. This finding further supports the notion that there is no measurable direct electron transfer from $Cu_A$ to the binuclear site that would bypass the low-spin heme (see also below).

Figure 4 (panels 4−6) shows the observed kinetic phases upon reacting the 3-electron-reduced $aa_3$ and $oa_3$ enzymes with $O_2$. The 1 ms spectrum (panel 4) is typical for formation of the **P** intermediate, which in this case is the $\mathbf{P_M}$ state in both enzyme populations due to the delayed transfer of an electron from $Cu_A$ to the binuclear site via heme *a* (and heme *o*). In the second phase ($\tau \sim 20$ ms, panel 5) the $\mathbf{P_M}$ state disappears with appearance of **F**. This event must occur in the $aa_3$ population, because disappearance of $\mathbf{P_M}$ in the $oa_3$ population occurs much later in time (panels 3 and 6).

Figure 5 shows the kinetics of membrane potential generation when fully reduced (trace 1) and approximately 3-electron-reduced R54M mutant enzyme (trace 2) reacts with $O_2$. In the fully reduced case a fast initial development of membrane potential (amplitude ~12.5 mV; see inset) is observed with a time constant ($\tau \sim 60$ $\mu$s) similar to that in the wild-type enzyme. This is followed by very slow $\Delta\psi$ development beyond the time scale shown here, which is best described as the sum of at least two phases. The summed amplitude of these slow phases is similar to that of the fast phase. Figure 6 (upper panel) summarizes our interpretation. The fast electrogenic phase can be ascribed to the conversion of the $\mathbf{P_R}$ intermediate to **F** and is kinetically the same as the analogous reaction for the wild-type enzyme. The $\mathbf{P_R}$ state is indeed expected to be formed at a normal rate in the mutant enzyme since heme *a* is reduced initially. This reaction might even be faster than in the wild-type enzyme due to the higher driving force that results from the low $E_{m,7}$ of heme *a* in the mutant, but this reaction has not been time-resolved in this study. The formation of $\mathbf{P_R}$ is not an electrogenic step, and therefore it yields no electrometric response, but it is seen as an initial lag (Figure 5, inset). The subsequent $\mathbf{P_R} \rightarrow$ F step does not involve electron transfer, but it is associated with net proton uptake (*24*−*26*) and proton translocation (*10*). Figure 5 (trace 1) shows that this step proceeds at a normal rate in the R54M mutant enzyme. However, the final reaction step ($\mathbf{F} \rightarrow \mathbf{O}$) is slowed

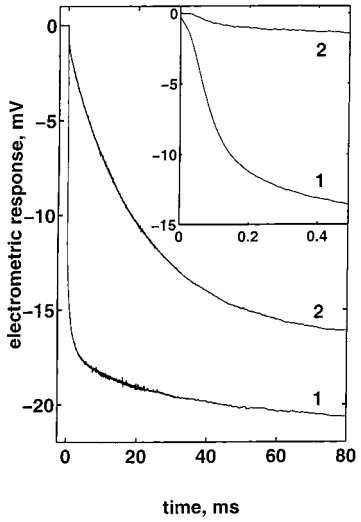


FIGURE 5: Generation of transmembrane electric potential during the reaction of the fully reduced and 3-electron-reduced R54M mutant enzyme with $O_2$. Trace 1: fully reduced cytochrome $aa_3$ (and 3-electron-reduced cytochrome $oa_3$; see text). Trace 2: approximately 3-electron-reduced cytochrome $aa_3$ (and $oa_3$). The inset shows the same curves on a shorter time span. Conditions: 0.1 M HEPES (pH 8), 50 mM glucose, 20 $\mu$M ruthenium(II) hexammine chloride, 0.12 mg/mL glucose oxidase, 12 $\mu$g/mL catalase, and 1 atm of CO. The laser flash was fired at $t = 0$.

about 20−50-fold relative to the wild-type enzyme. This is consistent with the fact that the **F** → **O** step involves transfer of the fourth electron from $Cu_A$ via heme *a* to the binuclear site, which is impeded in the mutant enzyme due to the low $E_{m,7}$ of heme *a*. These electrometric results are consistent with our observation that the mutation does not affect the efficiency of proton translocation but merely slows down electron transfer via heme *a*.

Due to the lowered $E_{m,7}$ of heme *a*, the mutant $aa_3$ enzyme can be successfully titrated to a 3-electron-reduced state, where $Cu_A$ and the binuclear site metals are reduced, but heme *a* remains oxidized (see above). In the 3-electron-reduced enzyme the reaction sequence after $O_2$ binding is truncated at intermediate **F**. Figure 5 (trace 2) shows the electrometric response for this reaction. Here, the first main electrometric phase has a time constant of ca. 12 ms and an amplitude of ca. 15 mV. This is followed by a much slower phase with small amplitude (beyond 100 ms; not shown), which probably results from a small fraction of fully reduced enzyme, the presence of which is also indicated by a low-amplitude fast blip in the beginning of the trace (Figure 5, inset). Figure 6 (lower panel) summarizes our interpretation. In the 3-electron-reduced enzyme heme *a* is the center that, in the main, remains oxidized due to its low $E_{m,7}$, which was confirmed by optical spectroscopy (Figure 4, panels 4 and 5). In this case, the binuclear site is expected to form intermediate $\mathbf{P_M}$ instead of $\mathbf{P_R}$ upon its reaction with $O_2$, due to the delayed transfer of the electron from $Cu_A$ via heme *a* to the binuclear site. Further conversion of $\mathbf{P_M}$ into intermediate **F** will be limited by the transfer of this third electron, and the corresponding electrogenic phase is indeed observed at a rate much slower than in the wild-type enzyme. The time-resolved optical data in Figure 4 (panel 5) confirm that the electrometric 12 ms phase indeed corresponds to the transition of $\mathbf{P_M}$ to **F**.

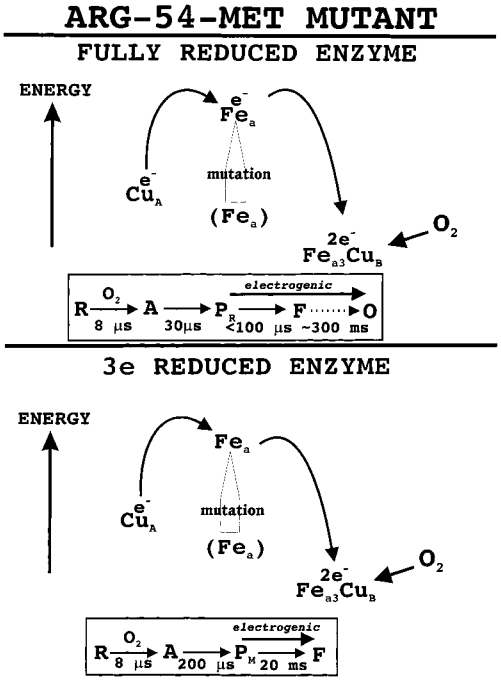


FIGURE 6: Reaction sequence. In the fully reduced case (upper panel), the binuclear center ($Fe_{a3}Cu_B$) is reduced by two electrons, and one electron each resides in heme *a* ($Fe_a$) and $Cu_A$ prior to the reaction with $O_2$. The R54M mutation is shown to increase the energy level of the electron in $Fe_a$ (lowered $E_{m,7}$). The reaction sequence indicates the 8 and 30 $\mu$s steps in which the reduced binuclear site (**R**) forms the oxygen adduct (**A**) and the $\mathbf{P_R}$ intermediate. Formation of $\mathbf{P_R}$ involves transfer of the electron in $Fe_a$ to the binuclear site, and this is unimpeded in the R54M mutant relative to the wild-type enzyme. Further conversion of $\mathbf{P_R}$ to **F** involves electrogenic proton transfer and proton translocation and takes place as in the wild-type enzyme. The final transition of **F** to **O** also generates membrane potential but requires transfer of the fourth electron in $Cu_A$ to the binuclear center. This step is slowed in the R54M mutant due to the thermodynamically unfavorable electron transfer via $Fe_a$. In the 3-electron-reduced case (lower panel), the low-potential $Fe_a$ remains oxidized. The reactions of the R54M mutant enzyme with $O_2$ are unimpeded until the $\mathbf{P_M}$ intermediate. Conversion of $\mathbf{P_M}$ to **F** requires that the electron in $Cu_A$ is transferred to the binuclear site via $Fe_a$ and is therefore considerably decelerated in the R54M mutant enzyme. While slow, this electrogenic step, which is associated with proton translocation, nevertheless creates about the same membrane potential as the step from $\mathbf{P_R}$ to **F** (see text).

These findings are consistent with our conclusion that the R54M mutation exerts its effect on the $aa_3$ enzyme purely by lowering the $E_{m,7}$ of heme *a*. A bypass of heme *a* and direct electron transfer from $Cu_A$ to the binuclear site, as suggested by Kannt et al. (*4*), is contradicted by the present results. We should reiterate that although the R54M mutant enzyme preparation contains about one-half cytochrome $oa_3$ in addition to cytochrome $aa_3$ (cf. ref *4*), heme *o* is not reduced prior to the reaction with $O_2$ in the flow-flash experiments reported here due to its very low $E_{m,7}$ value. While the **P** intermediate is formed also in the cytochrome $oa_3$ enzyme fraction in its reaction with $O_2$, the extent of the subsequent decay of the **P** state is only about one-half of the **P** formed initially (Figure 4, panels 4 and 5), which indicates that the reaction beyond **P** in the $oa_3$ enzyme fraction is too slow to be part of the reactions studied electrometrically here. In agreement with this, we find by optical spectroscopy that the second half of **P** (in the $oa_3$

enzyme) decays at an extremely slow rate that is far outside the present time regime (Figure 4, panels 3 and 6).

The extent of membrane potential generation associated with the 20 ms decay of the $\mathbf{P_M}$ intermediate to **F** in the 3-electron-reduced $aa_3$ enzyme is only approximately 20% larger than the amplitude by which membrane potential is formed in the fast transition of $\mathbf{P_R}$ into **F** in the reaction of the fully reduced mutant enzyme (Figure 5). This allows us to draw an important conclusion: The fully reduced enzyme is not impaired with respect to its capability of proton translocation, as recently suggested (*9*). In Michel's model the reactions from intermediate **A** to intermediate **F** were proposed to be associated with pumping of one proton across the dielectric when initiated from the fully reduced enzyme, but two protons were proposed to be pumped when the reaction occurs via the $\mathbf{P_M}$ intermediate (*9*). However, the comparable electrogenic amplitudes of the $\mathbf{P_R} \rightarrow \mathbf{F}$ and $\mathbf{P_M} \rightarrow \mathbf{F}$ transitions reported here show that an approximately equal number of electrical charges are translocated across the membrane in both cases. In fact, the ~20% larger amplitude associated with the latter transition can be accounted for by the electrogenic electron transfer from $Cu_A$ to the binuclear site, which does not occur during $\mathbf{P_R} \rightarrow \mathbf{F}$ in the mutant enzyme. It follows from this that the enzyme is quite robust with respect to its proton translocating mechanism, which functions normally also when initiated from the fully reduced state where the uptake of four electrons has not been fully charge-compensated by uptake of protons (*9*, *25*).

## ACKNOWLEDGMENT

We thank Marina L. Verkhovskaya for help with protein reconstitution and Katja Sissi for skillful technical assistance.

## REFERENCES

1. Brzezinski, P. (1996) *Biochemistry 35*, 5611−5615.
2. Babcock, G. T., and Wikström, M. (1992) *Nature 356*, 301−309.
3. Ferguson-Miller, S., and Babcock, G. T. (1996) *Chem. Rev. 7*, 2889−2907.
4. Kannt, A., Pfitzner, U., Ruitenberg, M., Hellwig, P., Ludwig, B., Mäntele, W., Fendler, K., and Michel, H. (1999) *J. Biol. Chem. 274*, 37974−37981.
5. Riistama, S., Verkhovsky, M. I., Laakkonen, L., Wikström, M., and Puustinen, A. (2000) *Biochim. Biophys. Acta 1456*, 1−4.
6. Lee, H.-m., Das, T. K., Rousseau, D. L., Millsa, D., Ferguson-Miller, S., and Gennis, R. B. (2000) *Biochemistry 39*, 2989−2996.
7. Babcock, G. T., and Callahan, P. M. (1983) *Biochemistry 22*, 2314−2319.
8. Oliveberg, M., and Malmström, B. G. (1992) *Biochemistry 31*, 3560−3563.
9. Michel, H. (1999) *Biochemistry 38*, 15129−15140.
10. Verkhovsky, M. I., Jasaitis, A., Verkhovskaya, M. L., Morgan, J. E., and Wikström, M. (1999) *Nature 400*, 480−483.
11. Riistama, S., Laakkonen, L., Wikström, M., Verkhovsky, M., and Puustinen, A. (1999) *Biochemistry 38*, 10670−10677.
12. Rigaud, J.-L., Pitard, B., and Levy, D. (1995) *Biochim. Biophys. Acta 1231*, 223−246.
13. Jasaitis, A., Verkhovsky, M. I., Morgan, J. E., Verkhovskaya, M. L., and Wikstrom, M. (1999) *Biochemistry 38*, 2697−2706.
14. Backgren, C., Hummer, G., Wikström, M., and Puustinen, A. (2000) *Biochemistry 39*, 7863−7867.
15. Drachev, L. A., Kaulen, A. D., Semenov, A. Yu., Severina, I. I., and Skulachev, V. P. (1979) *Anal. Biochem. 96*, 250−262.
16. Verkhovsky, M. I., Morgan, J. E., Verkhovskaya, M. L., and Wikström, M. (1997) *Biochim. Biophys. Acta 1318*, 6−10.
17. Gibson, Q. H., and Greenwood, C. (1963) *Biochem. J. 86*, 541−555.
18. Wikström, M., Jasaitis, A., Backgren, C., Puustinen, A., and Verkhovsky, M. I. (2000) *Biochim. Biophys. Acta 1459*, 514−520.
19. Farrar, J. A., Lappalainen, P., Zumft, W. G., Saraste, M., and Thomson, A. J. (1995) *Eur. J. Biochem. 232*, 294−303.
20. Gennis, R. B. (1998) *Biochim. Biophys. Acta 1365*, 241−248.
21. Yoshikawa, S., Shinzawa-Itoh, K., Nakashima, R., Yaono, R., Yamashita, E., Inoue, N., Yao, M., Fei, M. J., Libei, C. P., Mizushima, T., Yamaguchi, H., Tomizaki, T., and Tsukihara, T. (1998) *Science 280*, 1723−1729.
22. Pfitzner, U., Odenwald, A., Ostermann, T., Weingard, L., Ludwig, B., and Richter, O.-M. H. (1998) *J. Bioenerg. Biomembr. 30*, 89−93.
23. Morgan, J. E., Verkhovsky, M. I., and Wikström, M. (1996) *Biochemistry 35*, 12235−12240.
24. Oliveberg, M., Hallén, S., and Nilsson, T. (1991) *Biochemistry 30*, 436−440.
25. Mitchell, R., and Rich, P. R. (1994) *Biochim. Biophys. Acta 1186*, 19−26.
26. Brzezinski, P., and Ädelroth, P. (1998) *J. Bioenerg. Biomembr. 30*, 99−107.

BI002948B